



NIH PUBLIC ACCESS

Author Manuscript

Nat Mater. Author manuscript; available in PMC 2012 June 01.

Published in final edited form as:

Nat Mater. ; 10(12): 980–986. doi:10.1038/nmat3146.

Electrochemical Activation and Inhibition of Neuromuscular Systems through Modulation of Ion Concentrations with Ion-Selective Membranes

Yong-Ak Song^{1,2}, Rohat Melik^{1,2}, Amr N. Rabie^{3,4}, Ahmed M. S. Ibrahim³, David Moses⁵, Ara Tan⁶, Jongyoon Han^{1,2,*}, and Samuel J. Lin^{3,*}

¹Department of Electrical Engineering and Computer Sciences, Massachusetts Institute of Technology, Cambridge, MA

²Department of Biological Engineering, Massachusetts Institute of Technology, Cambridge, MA

³Divisions of Plastic Surgery and Otolaryngology, Beth Israel Deaconess Medical Center, and Harvard Medical School, Boston, MA

⁴Department of Otolaryngology, Ain Shams University, Cairo, Egypt

⁵Department of Bioengineering, Rice University, Houston, TX

⁶Department of Chemical Engineering, University of Minnesota, Twin Cities, MN

Conventional functional electrical stimulation (FES) aims to restore functional motor activity of patients with disabilities resulting from spinal cord injury or neurological disorders. However, FES-related intervention in neurological diseases lacks an effective, implantable method that suppresses unwanted nerve signals. We have developed an electrochemical method to activate and inhibit a nerve by electrically modulating ion concentrations *in situ* along the nerve. Using an ion-selective membrane (ISM) to achieve different excitability states of the nerve, we observe either a reduction of electrical threshold by up to approximately 40%, or voluntary, reversible inhibition of nerve signal propagation. This low-threshold electrochemical-stimulation method is applicable in current implantable neuroprosthetic devices, whereas the on-demand nerve blocking mechanism could offer an effective clinical intervention for chronic disease states caused by uncontrolled nerve activation, such as epilepsy and chronic pain syndromes.

The initiation and conduction of nerve impulses are based on the electrochemical processes localized in the surface structure of nerve cells and their axons¹, which was quantitatively described by the Hodgkin-Huxley model.² Roles of various ionic species (K⁺, Na⁺, and Ca²⁺) in the propagation of action potentials have been well characterized, both theoretically and experimentally. Extracellular potassium concentration largely determines the resting potential of axons, while the sodium concentration gradient is mainly responsible for the generation of action potentials. The role of calcium ions in nerve stimulation is known to be the gating of potassium ion channels.³ Local, temporary modulation of these ion concentrations would enable novel modes of control and manipulation of the nervous system, but such methods have never been realized in the context of prosthetic devices and *in vivo* situations. Based on the role of potassium, sodium, and calcium^{4, 5} ions in neural

*Co-corresponding Authors: Jongyoon Han (jyhan@mit.edu). Samuel J. Lin (sjlin@bidmc.harvard.edu).

Author Contribution Y.-A. S. performed fabrication of ion-selective electrodes and membranes, experimental work and confocal imaging. R. M., A. N. R., A. M. S. I., D. M., and A. T. conducted experimental work and data analysis. J. H. and S. J. Lin performed project planning. Y.-A. S., S. J. L., and J. H. wrote the manuscript.

processes, we developed an electrochemical method by using ion-selective membranes (ISMs) to modulate the ion concentration *in situ* to change the nerve excitability locally at the site of electrical stimulation for more efficient stimulation, or along the nerve fiber for more efficient on-demand suppression of nerve propagation. The K^+ , Na^+ , and Ca^{2+} ion concentration modulation was achieved by running small direct currents (10~100 times smaller than FES thresholds) through either K^+ , Na^+ or Ca^{2+} ion-selective membranes, therefore inducing local, dynamic, and selective depletion of target ions immediately juxtaposed to the nerve. Our approach is based on a microfabricated ISM and eliminates the requirement of a chemical reservoir in the implant with traditional chemical stimulation methods,^{6,7} significantly simplifying system design and operation. These ions are naturally present in the interstitial fluid near the nervous system *in vivo*.

Enhancing neuromuscular stimulation with Ca^{2+} ISMs

For *in vitro* experiments, we placed a sciatic nerve (with perineurium and epineurium preserved) on a microfabricated planar gold electrode array and stimulated the nerve electrically (Figure 1). Details about the fabrication of ion-selective microelectrodes and preparation of frogs are given in Methods section. First, we applied an ion depletion current i_d across the ion-selective membrane between two diametrically opposite electrodes in the center, as shown schematically in Figure 2a. We limited the ion depletion current i_d to $1 \mu A$, which was well below nominal current thresholds for electrical stimulation. The planar microelectrode covered with the ion-selective membrane acted as a cathode and the opposite electrode as an anode to deplete the positively charged Ca^{2+} ions. After depleting the ions at a given current i_d for duration t_d , we applied an electrical stimulus current i_s between the two outer stimulating electrodes and the center contact electrode (covered with the Ca^{2+} ion-selective membrane) while i_d across the ion-selective membrane was off (Figure 2b). Stimulation threshold currents, as well as resulting muscle contraction force originating from the stimulation were simultaneously measured and compared between conditions (see Methods section).

In all tests, we first measured the electrical current stimulation threshold using bare gold electrodes without ion depletion or modulation. While there was a variation between different animal preparations, we used a standard pulse train between $i_s = 2$ and $20 \mu A$ at a pulse width of $t_p = 300 \mu s$ or $1 ms$ and a pulse frequency of $f = 1 Hz$. Using a microfabricated Ca^{2+} ion-selective membrane on the sciatic nerve of a frog, we achieved a decrease of the electrical threshold value from $7.4 \mu A$ down to $4.4 \mu A$ (approximately 40% decrease) without applying any ion depletion current i_d prior to stimulation, as shown in Figure 3. This reduction of threshold was achieved solely based on the stimulus current i_s , which triggered Ca^{2+} ion depletion and electrical stimulation simultaneously. To lower the threshold further, we first applied a depletion current of $i_d = 1 \mu A$ across a Ca^{2+} ion-selective membrane for $t_d = 1 min$ and then applied a stimulation electrical pulse i_s directly thereafter. In this way, we could decrease the threshold down to $2.2 \mu A$. These measurements were repeated at least 4 times in different animal preps, and we achieved an average reduction of the threshold by ~40 percent with direct ISM stimulation, and an additional 20 percent with 1 min Ca^{2+} depletion before stimulation was achieved.

In Figure 4a, we systematically investigated the influence of ion depletion time i_d on the threshold. As a control experiment to verify the effect of Ca^{2+} ion depletion on nerve excitability, we also used PVC (polyvinyl chloride) membranes without Ca^{2+} ion-specific ionophore. As shown in Figure 3, the Ca^{2+} ion-selective membrane allowed a decrease in the threshold value directly without applying an additional ion depletion current ($t_d = 0 min$), simply by utilizing the stimulus current flowing into the cathode for Ca^{2+} ion depletion. If an additional ion depletion current $i_d = 1 \mu A$ is applied prior to stimulation for

t_d 1–3 min, we could observe a further decrease of the threshold value as a function of depletion time t_d . In a control experiment with the PVC membrane,^{8,9} there was no noticeable decrease of the threshold value when stimulating without ion depletion current i_d applied prior to stimulation. When applying i_d , however, we could also observe a continuous decrease of the threshold as a function of ion depletion time t_d . This result indicates that the sub-threshold current i_d applied between the two center electrodes also increased axonal excitability. However, the amount of net threshold reduction was ~10% higher in the case of the Ca^{2+} membrane from $t_d=0$ to $t_d=1$ min. It is evident from this result that there are two coupled effects influencing axonal excitability: 1) the effect of sub-threshold DC current leading to electrotonus^{10,11} and 2) the effect of Ca^{2+} ion depletion. A stimulation experiment with ISM in 10% donkey serum showed that our device could also work in a serum-rich environment such as body fluid.

When switching the polarity of the electrodes (ISM on the anode vs. cathode), we also observed a decrease of the threshold, as shown in Figure 4b. This result confirmed that the sub-threshold current i_d contributes to a decrease of the threshold in addition to the Ca^{2+} ion concentration modulation. When we compared the final reduction ratios of both polarities, the ion depletion mode with the ISM on the cathode was more effective by ~10% up to $t_d=2$ min after offsetting the initial difference of the reduction ratios at $t_d=0$ min (p value of 0.0133). As shown in Figure 4c, the amount of decrease in the threshold value was dependent on the amount of ion depletion current i_d . At $i_d=100\text{nA}$ and 10nA , no significant reduction of the threshold could be achieved when depleting longer than $t_d=1$ min (p value of 0.0107). Based on these data, an estimation of energy expenditure for our electrochemical stimulation method is given in comparison with FES in Supplementary Data.

The storing capacity of the ion-selective membrane printed on the microfabricated electrode will be limited due to its finite thickness (typically 5–20 μm). The duration of depletion current as well as its amplitude will define the amount and speed of ion depletion from the nerve into the pores of the membrane. However, once the ion reservoir capacity of the membrane has been reached, it is likely that the effect of ion depletion on the electrical stimulus threshold will no longer be present due to the steady state of ionic concentration, and eventually, the ionic concentrations are restored to their normal level due to homeostasis. To “empty” the ion reservoir, the polarity of the electrodes needs simply to be reversed. A potential solution to address this issue of limited ion storage capacity in the membrane is designing a stimulation device, where ion-selective membrane material is used as a ‘filter’ rather than ‘storage’ of the particular ion (see Supplementary Figure 1).

Our *in vitro* experimental results using a microfabricated planar ISM, as well as a conventional ISM in the form of a glass pipette tip (see details about the fabrication of ion-selective pipette tips in Methods section and experimental results in Supplementary Figures 2–5), demonstrate that the depletion of Ca^{2+} ions can reduce the electrical threshold value by approximately 40% without a constant perfusion and approximately 20% under a constant perfusion of Ringer's solution. With a microfabricated ISM, we demonstrated that a Ca^{2+} ion-selective membrane layer printed with a thickness of 5–20 μm on a planar microelectrode can be used as a selective ion reservoir to deplete and store the target ion from a zone adjacent to the nerve by controlling the potential/current across the ISM. To the best of our knowledge, this is the first time that a local *in situ* control of ion concentration has been utilized to achieve higher excitable states for electrical stimulation. This significant reduction of the electrical threshold value could be achieved at a depletion current of i_d 1 μA (usually less than 2V applied across the ion-selective membrane to maintain the ion depletion current in the microfabricated electrodes). It is likely that one can increase the efficacy of this method (in terms of speed and threshold reduction) by utilizing higher ion depletion currents. Nonetheless, water is hydrolyzed at electrode potentials over

approximately 2V, and above this voltage chlorine ions can be oxidized at the electrode surface potentially producing toxic compounds limiting application potential. To overcome this limitation, we can further decrease the gap size between the electrodes (currently 200 μm).

We confirmed the role of Ca^{2+} ions in nerve excitation in a separate control experiment where the nerve was completely immersed in a Ca^{2+} ion depleted Ringer's bath solution (see Supplementary Figure 6). In this context, an important point to consider is whether the isotonic Ringer's solution used in our *in vitro* experiment is representative for the extracellular fluid *in vivo*. Ringer's solution as an isotonic solution with a similar ionic composition to that of the extracellular fluid is widely used in the study of peripheral nerve excitability.¹² The fact that the perineurium acts as a diffusion barrier to proteins and small molecules^{13,14,15} and thereby reduces the influence of proteins and molecules on nerve excitability also supports the use of Ringer's solution in our experiments. The only difference regarding the use of the extracellular fluid versus Ringer's solution is that the presence of proteins and other molecules might have an impact on the lifetime of the ion-selective membranes due to non-specific binding. Furthermore, we demonstrate that the force amplitude generated at the downstream muscle can be more accurately controlled by the Ca^{2+} ion depletion. This result implies that controlling muscle contraction is possible with a higher degree of resolution and/or dynamic range than with traditional FES methods. It is hypothesized that the graded response of downstream muscle contraction may be due to the local manner of perturbing Ca^{2+} ion concentration (modulating ion concentration on one side of a fiber).

Nerve conduction blocking with Ca^{2+} ISMs

Another important application of our ISM device is nerve conduction blocking. To investigate whether a modulation of the Ca^{2+} ion concentration along the nerve is an effective way of lowering the blocking threshold of the nerve signal conduction, we positioned an ISM device between the site of stimulation and the muscle in a bipolar, perpendicular configuration (Figure 5). The anode was positioned closer to the proximal stimulating electrodes than the two cathodes. The direct current block of peripheral nerves is previously demonstrated by several groups.^{16,17} The Kilgore group reported a mean direct current of $\sim 50 \mu\text{A}$ required to block the nerve signal in a frog sciatic nerve with spiral-shaped wires wrapped around the sciatic nerve at least 5 times.¹⁸ Applying high-frequency AC current was also previously reported as one potential method for nerve conduction block.¹⁹ This method enabled a rapidly reversible nerve conduction block in animal models.¹⁸ In the frog, a sinusoidal or rectangular waveform (3–5 kHz and 0.5–2 $\text{mA}_{\text{p-p}}$) allowed the most consistent block.²⁰ However, no implant device has been demonstrated based on this approach so far.^{19,20,21} Compared to the electrodes without ISM (Figure 5a), the planar microelectrodes with a surface-printed Ca^{2+} ion-selective membrane enabled a 25–50% reduction of DC block threshold from $i_b=50\text{--}100 \mu\text{A}$ to $10\text{--}50 \mu\text{A}$ in 13 experiments (Figure 5b). We could modulate the transmitted nerve signal by varying the amount of the DC block current applied. In addition, recovery to the previous twitch amplitude was almost instantaneous after turning off the DC current.

Nerve block caused by Na^+ and K^+ ion depletion

In addition to the Ca^{2+} ion-selective membrane, we also tested a Na^+ ion-selective membrane deposited on the cathode in the same device ('perpendicular geometry'). The hypothesis was that depleting extracellular Na^+ ions would lead to action potential block by eliminating the driving force behind action potential generation, but we could not achieve any significant decrease of the blocking threshold. This finding may be due to the fact that

extracellular Na^+ ion concentrations are generally high (requiring a much significantly higher perturbation current), and that Na^+ depleted regions may be too short to overcome the 'safety factor' of the nerve action potential propagation. With a surface contact length of 10mm between the membrane and the nerve for Na^+ ion depletion ('parallel geometry' in Supplementary Figure 7a), we achieved a graded blocking of the sciatic nerve for an electrical stimulus by depleting the Na^+ ions from the nerve and its surroundings without continuous perfusion of Ringer's solution (Supplementary Figure 7b). No muscle response was recorded even at higher electrical pulses with i_s over $30 \mu\text{A}$ after depleting Na^+ ions for 5 min with $i_d = 1 \mu\text{A}$ across the Na^+ ion-selective membrane when the twitch amplitude before the blocking was in the range of $\sim 1\text{mN}$. At higher twitch amplitudes ($\sim 100\text{mN}$), however, a significantly larger ion depletion current was required between $i_d = 50\text{--}100 \mu\text{A}$ to observe blocking after 5 min of Na^+ ion depletion. To investigate the reversibility of the signal blocking method by Na^+ ion depletion, we discontinued the ion depletion current and immersed the nerve with Ringer's solution. Recovery to the original nerve excitability state required approximately 10 minutes in Ringer's solution. We also observed a similar blocking effect when modulating the K^+ ion concentration with a K^+ ion-selective pipette tip (see Supplementary Figure 8 and Figure 9). It appeared that injecting K^+ ions from the pipette tip filled with 100mM KCl solution onto the nerve was more effective in terms of nerve signal blocking than depleting these ions under continuous perfusion of Ringer's solution, which is expected since the incubation of a nerve in high K^+ concentration leads to the elimination of potassium concentration gradient across the membrane, and therefore membrane potential.

Nerve blocking by Na^+ and K^+ depletion demonstrated limited reversibility. To restore the excitability of the nerve after blocking, incubation with Ringer's solution or a significant time delay were necessary, which is in contrast with the almost immediate reversibility of Ca^{2+} ion depletion based blocking. Potassium ion concentration gradient across the membrane is the main determinant of the membrane resting potential. Therefore, significant modification of the K^+ concentration near the nerve could shift the resting potential, possibly inducing currents along the nerve. This concept may explain the 'difficulty' of regaining ion homeostasis. When using a cation-selective membrane such as Nafion with a reversed polarity of the ISM (the Nafion membrane deposited on the anodic side), which creates a general ion depletion zone (depletes all ions), we also achieved a similar blocking effect (Supplementary Figure 10). This nerve blocking state could be reversed by immersing the nerve in a bath of Ringer's solution for 10 min (see Supplementary Figure 11). We repeated this cycle of inhibition and relaxation for three times with an immersion of the nerve in Ringer's solution for 10 min between each cycle. In addition to Nafion, we could potentially achieve a similar effect with other cation-selective membrane materials such as poly(3,4-ethylenedioxythiophene) doped with poly(styrene sulphonate) (PEDOT:PSS) which, as an electrically conducting organic polymer, was previously used to demonstrate electronic control of the ion homeostasis in neurons.²²

One key constraint that could limit the effectiveness of our approach is the permeability of the perineurium for ions. The perineurium constitutes a diffusion barrier to electron-dense tracers^{23,24} and to small ions.^{25,26,27} Consequently, there is a lag in the change of nerve excitability as a result of to the change of ion concentrations in the extracellular fluid.²⁸ Also, depending on the diameter of the nerve, the majority of axons could be insensitive to the local ionic manipulation. Our confocal imaging data showed that a change of ionic concentration due to ISM was limited to $\sim 120\mu\text{m}$ inside the nerve fiber (see details about confocal imaging in Methods section and results in Supplementary Figure 12). In order to translate these ideas to various neural prosthetic devices, longer-term, *in vivo* reliability and safety studies need to be performed. Electrochemical reduction/oxidation processes at the electrodes, as well as any pH changes at the ion-selective membranes could be undesirable since they may alter the chemical composition of the extracellular fluid, producing cytotoxic

compounds and effects.²⁹ The pH shift at a current density of $10\mu\text{A}/\text{mm}^2$ seems to be of lesser concern for our experiments since the Ringer's solution was adequately buffered.³⁰ In these ion-selective membranes, since the current density was significantly lower with $318\text{nA}/\text{mm}^2$ for the ion-selective pipette electrode and $\sim 5\mu\text{A}/\text{mm}^2$ for the planar ion-selective electrodes, we would expect fewer problems with pH shift. Regarding the nerve blocking effect, ISMs in combination with AC current²¹ could potentially lower the blocking threshold in a similar manner as the DC current.

In sum, we have demonstrated a novel means of using ion-selective membranes in modulating the activation and inhibition of nerve impulses in a reversible, graded fashion. These findings have potentially significant implications for the design of low-power, compact, neural prosthetic devices that selectively enhance nerve action potentials or inhibit unwanted motor endplate action potentials or noxious nerve stimulation. The devices demonstrated in this paper are readily applicable as electrochemical nerve manipulation technology, entirely *controlled electrically* without the need for chemical (ion) reservoirs and other complicated setup. We envision that these types of electrodes can be fabricated on a flexible substrate³¹ without any modification, for better enmeshing and contouring for nerve fibers and cells of various shapes and sizes. In this method, the ion depletion time could be significantly reduced because of increased surface contact area between the nerve and electrodes. With a projected flexible electrode system wrapped around the nerve, it is expected that one could achieve an even greater control of nerve excitability. Further studies will be conducted to find out whether this electrochemical stimulation technique can be extended to mammalian nerves. Finally, given the broad roles of ions such as Ca^{2+} in cellular signaling, the use of ion selective membranes demonstrated in this work could be utilized to directly control important ionic species near biological tissues and cells.

Methods

Fabrication of ion-selective planar microelectrodes

The planar microelectrodes were fabricated using the standard lift-off process. In brief, we patterned a $1\mu\text{m}$ thick positive photoresist spin-coated on a 1mm thick glass wafer photolithographically. After depositing a 50nm Ti and 200nm Au layer on the patterned glass wafer using the e-beam deposition, the photoresist layer was removed in acetone overnight. Before depositing an ion-selective membrane, the electrode was dehydrated at 90°C on a hotplate for 24h and then silanized with N, N-dimethyltrimethylsilylamine (Fluka Inc.) for 60 min.³² To deposit/print an ion-selective membrane on top of a planar microelectrode, we placed a polydimethylsiloxane (PDMS) microchip with a single microfluidic channel ($300\text{--}1500\mu\text{m}$ wide and $50\mu\text{m}$ deep) and sealed it against the planar electrode after an optical alignment using a stereomicroscope. The ion-selective membrane for each specific ion was made using commercially available ion-selective cocktails from Sigma Aldrich Inc., potassium ionophore I for K^+ ion, sodium ionophore I for Na^+ ion and ETH124 (calcium ionophore II) for Ca^{2+} ion, in a plasticized amorphous polymer matrix such as polyvinyl chloride (PVC). The ion selective membrane was composed according to methods published.^{8,9,32} Using capillary force, the ion-selective resin mixture (10–20 wt. % for Ca^{2+} ionophore, 20 wt. % for K^+ and Na^+ ionophores in a plasticized amorphous matrix consisting of 35.8mg polyvinyl chloride in 0.4 mL cyclohexanone) was filled into the microchannel. The PDMS channel was immediately removed once the electrode has been covered with the ion-selective resin and the electrodes were stored in a darkroom and dried for 12 hours under ambient conditions. To deposit cation-selective membrane on the planar electrodes, we used Nafion perfluorinated resin solution with 20 wt. % in mixture of lower aliphatic alcohols and water (Sigma Aldrich Inc.)

Fabrication of ion-selective pipette tips

The ISM construct consisted of an ion-selective membrane at the top of an electrolyte solution (either 100mM CaCl₂ or 100mM KCl depending on the ion species to modulate)-filled glass pipette or PVC tip with one silver wire (127 μm OD) located inside and a second one outside the pipette tip. To enhance the adhesion of the ion-selective resin to the glass pipette surface, the pipettes were dehydrated at 90°C on a hotplate for 24 hours and then silanized with N, N-dimethyltrimethylsilylamine (Fluka Inc.) for 60 min.³² The ISM components were dissolved in 0.4 mL cyclohexanone (Fluka Inc.). The membrane resin was pipetted 2 mm into a glass pipette with an OD of 1.5 mm and ID of 0.8mm (World Precision Instruments Inc.). The height of the resin inside the pipette was controlled to 2mm and dried for 24 h under ambient conditions.

Frog preparation

North American bullfrogs (*Rana catesbeiana*) were purchased from Connecticut Valley Biological Supply Company. Their size was 5”–6”. Each acquired frog from Animal Facilities was sedated with 0.1–0.2 wt% MS222 (Ethyl 3-aminobenzoate, methanesulfonic acid) for about 30 min. or until the frog was no longer mobile. This protocol was approved by the Massachusetts Institute of Technology CAC. Preparation of nerves and gastrocnemius muscles is described in Supplementary Information.

Measurement of muscle contractile force, compound action potential and ion depletion/injection current

The end of the gastrocnemius muscle was attached to a dual range force transducer FT-302 (iWorx Inc.) via string. The force was recorded with a four channel data recorder (iWorx 214) and analyzed with LabScribe2 software. We used a standard Ringer's solution to keep the nerve and the muscle hydrated. In addition to the muscle contraction force, we also measured the compound action potential with a home-made amplifier and a PC-based oscilloscope. The ion depletion/injection current was applied with a dual-channel system sourcemeter 2612 from Keithley Inc.

Confocal imaging

We used a Fluo-4 NW calcium assay kit (F36206, Invitrogen) to measure the Ca²⁺ ion concentration change inside the sciatic nerve. We added 2.5 mL of assay buffer and 100μL of probenecid to Fluo-4 NW dye mix to obtain 10mM probenecid concentration. We immersed a 10mm long fresh sciatic nerve into Fluo-4 NW solution and maintained a 2 hour immersion time to let the nerve saturated with Fluo-4 dye. For confocal imaging, we used a Zeiss confocal microscope (LSM 710). To observe the sciatic nerve while depleting ions, we used a planar microelectrode composed of transparent ITO (indium-tin-oxide) deposited to a layer thickness of 100nm via a sputtering process. The electrodes were 10mm long and 750μm wide. A sciatic nerve was positioned on top of the Ca²⁺ ion-selective membrane for confocal imaging, as shown in Supplementary Figure 12a. For measurement of the fluorescence intensity in the confocal microscope, we increased the z height by 6.17μm from the bottom of the device into the sciatic nerve. More details about the experimental setup and imaging data are given in Supplementary Data.

Supplementary Material

Refer to Web version on PubMed Central for supplementary material.

Acknowledgments

This work was conducted with support from a MIT faculty discretionary research fund, a Harvard Catalyst Grant from the Harvard Clinical and Translational Science Center (NIH Award #UL1 RR 025758), and financial contributions from Harvard University and its affiliated academic health care centers.

References

1. Katz, B. Society of Experimental Biology Symposia 4. Structural Aspects of Cell Physiology 16–38. Cambridge University Press; Cambridge: 1952.
2. Hodgkin AL, Huxley AF. A quantitative description of membrane current and its application to conduction and excitation in nerve. *Journal of Physiology*. 1952; 117:500–544. [PubMed: 12991237]
3. Kandel, ER.; Schwartz, JH.; Jessell, TM. McGraw-Hill; 2000.
4. Brink F. The role of calcium ions in neural processes. *Pharmacological Reviews*. 1954; 6:243–298. [PubMed: 13215068]
5. Brink F, Bronk DW, Larrabee MG. Chemical excitation of nerve. *Annals of New York Academy of Sciences*. 1946; 47:457–485.
6. Santini JT, Cima MJ, Langer R. A controlled-release microchip. *Nature*. 1999; 397:335–338. [PubMed: 9988626]
7. Chen, J.; Wise, KD. Solid-State Sensor and Actuator Workshop, 256–259. Cleveland Heights; Ohio: 1994.
8. Ammann D, Buehrer T, Schefer U, Mueller M, Simon W. Intracellular neutral carrier-based Ca^{2+} microelectrode with subnanomolar detection limit. *Pfluegers Archiv*. 1987; 409:223–228. [PubMed: 3627942]
9. Baudet S, Hove-Madsen L, Bers DM, Nuccitelli R. Ch. 4. *Methods in Cell Biology*. 1994; Vol. 40
10. Bostock H, Cikurel K, Burke D. Threshold tracking techniques in the study of human peripheral nerve. *Muscle Nerve*. 1998; 21:137–158. [PubMed: 9466589]
11. Bostock H, Grafe P. Acitivity-dependent excitability changes in normal and demyelinated rat spinal root axons. *Journal of Physiology*. 1985; 365:239–257. [PubMed: 4032313]
12. Ask P, Levitan H, Robinson PJ, Rapoport SI. Peripheral nerve as an osmometer: role of the perineurium in frog sciatic nerve. *Am J Physiol*. 1983; 244:C75–81. [PubMed: 6600373]
13. Weerasuriya A, Spangler RA, Rapoport SI, Taylor RE. AC impedance of the perineurium of the frog sciatic nerve. *Biophys J*. 1984; 46:167–174. [PubMed: 6332648]
14. Bradbury MW, Crowder J. Compartments and barriers in the sciatic nerve of the rabbit. *Brain Res*. 1976; 103:515–526. [PubMed: 1252941]
15. Abbott NJ, Mitchell G, Ward KJ, Abdullah F, Smith IC. An electrophysiological method for measuring the potassium permeability of the nerve perineurium. *Brain Res*. 1997; 776:204–213. [PubMed: 9439814]
16. Petruska JC, Hubscher CH, Johnson RD. Anodally focused polarization of peripheral nerve allows discrimination of myelinated and unmyelinated fiber input to brainstem nuclei. *Experimental Brain Research*. 1998; 121:379–390.
17. Manfredi M. Differential block of conduction of large fibers in peripheral nerve by direct current. *Archives of Italian Biology*. 1970; 108:52–71.
18. Bhadra N, Kilgore KL. Direct current electrical conduction block of peripheral nerve. *IEEE Trans Neural Syst Rehabil Eng*. 2004; 12:313–324. [PubMed: 15473193]
19. Tanner JA. Reversible blocking of nerve conduction by alternating-current excitation. *Nature*. 1962; 195:712–713. [PubMed: 13919574]
20. Kilgore KL, Bhadra N. Nerve conduction block utilising high-frequency alternating current. *Med Biol Eng Comput*. 2004; 42:394–406. [PubMed: 15191086]
21. Bhadra N, Kilgore KL. High-frequency nerve conduction block. *Conf Proc IEEE Eng Med Biol Soc*. 2004; 7:4729–4732. [PubMed: 17271365]
22. Isaksson J, et al. Electronic control of Ca^{2+} signalling in neuronal cells using an organic electronic ion pump. *Nat Mater*. 2007; 6:673–679. [PubMed: 17643105]

23. Olsson Y, Reese TS. Permeability of vasa nervorum and perineurium in mouse sciatic nerve studied by fluorescence and electron microscopy. *J Neuropathol Exp Neurol.* 1971; 30:105–119. [PubMed: 5542492]
24. Waggener JD, Bunn SM, Beggs J. The diffusion of ferritin within the peripheral nerve sheath, an electron microscopy study. *J Neuropathol Exp Neurol.* 1965; 24:430–443.
25. Feng TP, Liu YM. The connective tissue sheath of the nerve as effective diffusion barrier. *J Cell Physiol.* 1949; 34:1–16. [PubMed: 15391939]
26. Krnjevic K. The distribution of Na and K in cat nerves. *J Physiol.* 1955; 128:473–488. [PubMed: 13243343]
27. Seneviratne KN, Weerasuriya A. Nodal gap substance in diabetic nerve. *J Neurol Neurosurg Psychiatry.* 1974; 37:502–513. [PubMed: 4276085]
28. Weerasuriya A. Permeability of endoneurial capillaries to K, Na and Cl and its relation to peripheral nerve excitability. *Brain Res.* 1987; 419:188–196. [PubMed: 3499951]
29. Prodanov D, Marani E, Holsheimer J. Functional electric stimulation for sensory and motor functions: progress and problems. *Biomedical Reviews.* 2003; 14:23–50.
30. Mortimer, J. *Handbook of Physiology - The Nervous System II* eds JM Brookshart & VB Mountcastle. American Physiology Society; 1981.
31. Kim DH, et al. Stretchable and foldable silicon integrated circuits. *Science.* 2008; 320:507–511. [PubMed: 18369106]
32. Guenat OT, et al. Microfabrication and characterization of an ion-selective microelectrode array platform. *Sensors and Actuators B-Chemical.* 2005; 105:65–73.

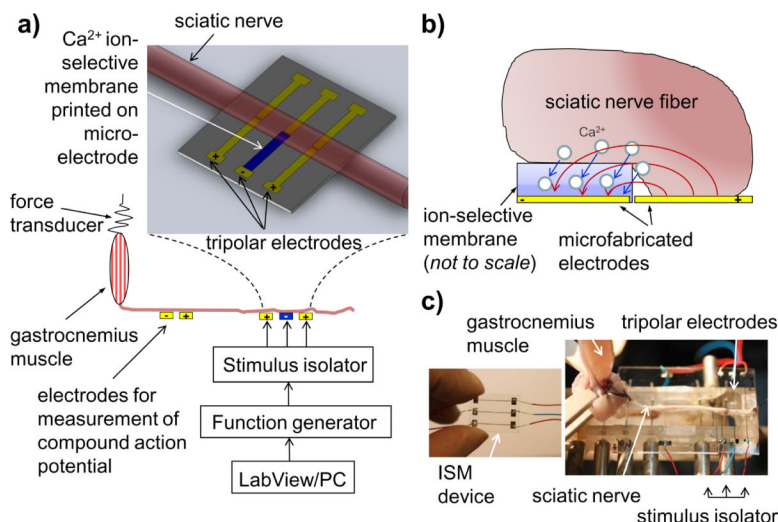


Figure 1. Principle and experimental setup of functional electrochemical stimulation with in-situ ion concentration modulation via ion-selective membranes. a) Schematic diagram of the experimental setup with a planar tripolar ISM electrode array for electrochemical stimulation of frog sciatic nerves with data acquisition of muscle contractile forces and compound action potentials. b) Schematic view of a Ca^{2+} ion-selective membrane surface-printed on top of a planar microelectrode. When applying direct current across two adjacent planar microelectrodes, the positively charged Ca^{2+} ions in the nerve become depleted locally near the membrane resulting in higher excitability for electrical stimulation. Using a microfabrication technique, the distance between the two electrodes as well as the thickness of the surface-printed ion-selective membrane can be precisely controlled. c) Experimental setup for stimulation of frog sciatic nerve with a Ca^{2+} ion-selective ISM device.

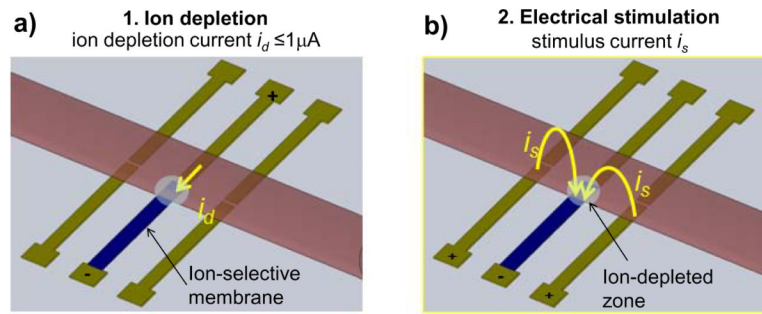


Figure 2. Operation modes of electrochemical stimulation with modulation of the local ion concentration adjacent to a nerve. a) In the ion depletion mode, Ca^{2+} ions are depleted from the stimulating electrode by applying an ion depletion current i_d of $1\mu\text{A}$ for $t_d=0-3$ min across the Ca^{2+} ion-selective membrane between two center electrodes. The depletion current i_d is at least one order of magnitude lower than the electrical threshold value i_s required for electrical stimulation. b) After depleting the ions at a given current i_d between the center electrodes at a distance of $200\mu\text{m}$ for duration t_d , stimulus current i_s is injected from the two outer stimulating electrodes into the center electrode covered with a several micron thin ($5-20\mu\text{m}$) Ca^{2+} ion-selective membrane while i_d across the ion-selective membrane was off.

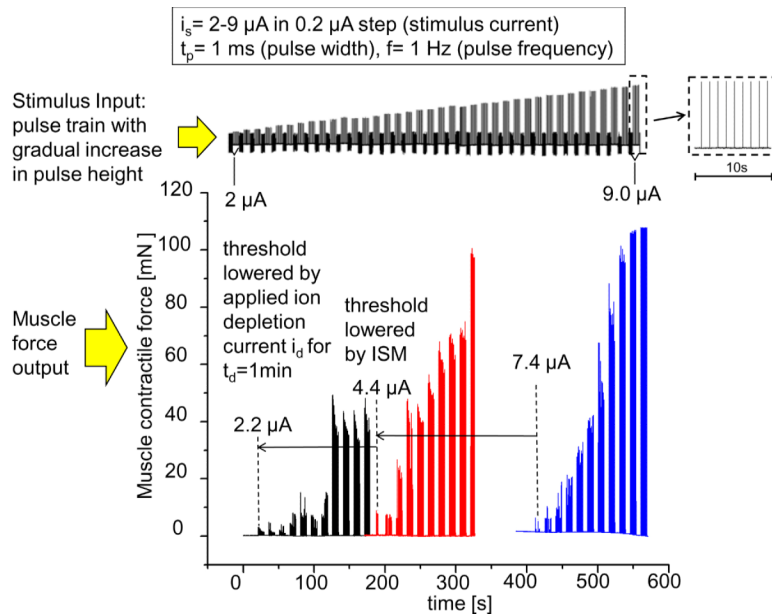


Figure 3.

Comparison of excitability without and with modulating Ca^{2+} ion concentration at an electrical current pulse train from $2\mu\text{A}$ to $9\mu\text{A}$, a pulse width of $t_p=1\text{ms}$, and a pulse frequency of $f=1\text{Hz}$. The minimum electrical current required to elicit a muscle contraction was lowered down from $i_s=7.4\mu\text{A}$ (plot in blue) to $4.4\mu\text{A}$ (plot in red) when directly stimulating with a Ca^{2+} ion-selective membrane deposited on the cathode without any prior ion depletion current (at $t_d=0$). When applying ion depletion current $i_d=1\mu\text{A}$ for $t_d=1\text{min}$ prior to stimulation, we could further reduce the threshold down to $2.2\mu\text{A}$ (plot in black).

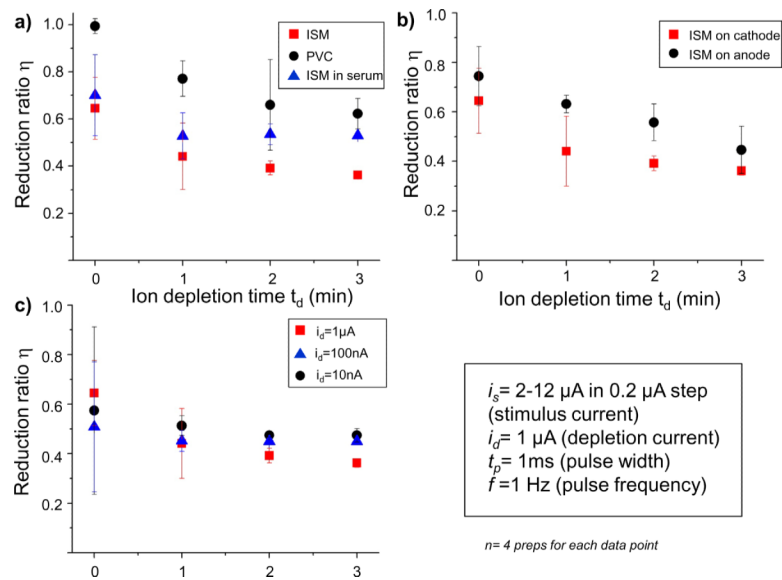


Figure 4.

Characterization of the electrochemical stimulation device under various parametric conditions. a) Comparison of the reduction ratios in Ringer's and serum environment. The reduction ratio is defined as $\eta = (\text{threshold with ISM} / \text{threshold without ISM})$. The control experiment was performed with a PVC membrane without Ca^{2+} ion-specific ionophore. For each data point, four different preps were used. b) Influence of the polarity on the reduction ratio. It is evident that the reduction of the threshold was caused by two effects: sub-threshold current i_d as well as Ca^{2+} ion depletion leading to higher axon excitability. c) Effect of the amount of ion depletion current i_d on the reduction ratio η . Increasing ion depletion current i_d enhanced axonal excitability due to higher subthreshold current as well as higher ion depletion simultaneously.

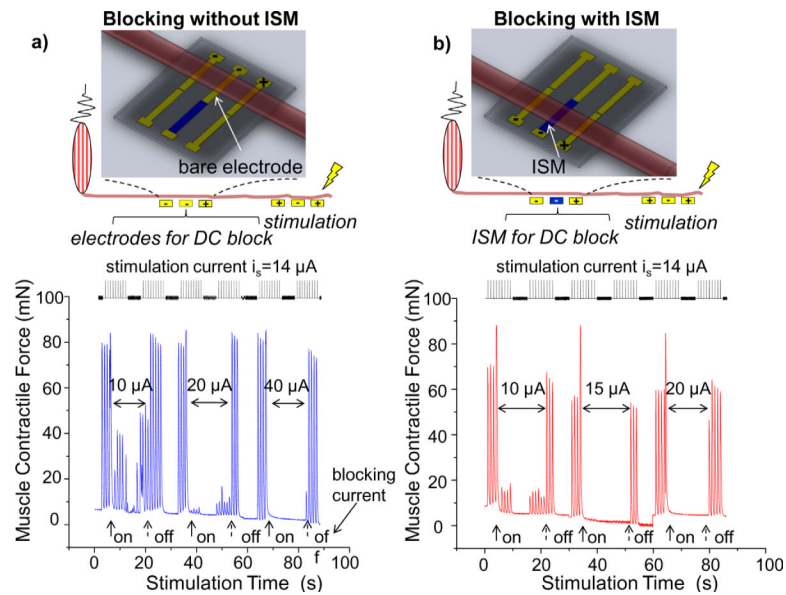


Figure 5. Nerve conduction block experiment with microfabricated ion-selective membrane device. a) Schematic of the setup for a study of the effect of ion concentration modulation on the DC nerve block. A single microfabricated ISM electrode array was positioned between the tripolar electrodes for electrical stimulation and the gastrocnemius muscle. First, the nerve was placed on top of the bare electrodes without ion-selective membrane. The anode facing the stimulation site first was followed by two cathodes. At a DC block current of $i_b = 10 \mu\text{A}$, we could achieve a partial blocking and at a DC block current of $i_b = 40 \mu\text{A}$, a total blocking. b) Application of nerve conduction block with a Ca^{2+} ion-selective membrane on the cathode. When using the Ca^{2+} ISM, we could lower the DC block threshold down to $i_b = 20 \mu\text{A}$. The nerve regained its twitch amplitude almost immediately after turning off the DC block current.